DTU Library

Mean load effects on the fatigue life of offshore wind turbine monopile foundations

Blasques, José Pedro Albergaria Amaral; Natarajan, Anand

Link back to DTU Orbit

MEAN LOAD EFFECTS ON THE FATIGUE LIFE OF OFFSHORE WIND TURBINE MONOPILE FOUNDATIONS

J.P. BLASQUES and A. NATARAJAN

Department of Wind Energy. Technical University of Denmark
Frederiksborgvej 399, 4000 Roskilde, Denmark
e-mail: jpbl@dtu.dk, anat@dtu.dk

Key words: fatigue damage, offshore wind turbine, monopile foundation, mean load correction

Abstract. This paper discusses the importance of mean load effects on the estimation of the fatigue damage in offshore wind turbine monopile foundations. The mud line bending moment time series are generated using a fully coupled aero-hydro-elastic model accounting for non-linear water waves and sea current. The fatigue damage is analysed in terms of the lifetime fatigue damage equivalent bending moment. Three different mean value correction techniques are considered, namely, Goodman, Walker, and mean sensitivity factor. An increase in the lifetime fatigue damage equivalent bending moment between 6% (mean sensitivity factor) and 33% (Goodman) is observed when mean load corrections are considered. The lifetime damage equivalent bending moment is further increased by approximately 7% when considering sea current forces. The results indicate that mean load correction techniques should be employed in the analysis of the fatigue life of offshore wind turbine monopile foundations. Moreover, it is shown that a nonlinear hydrodynamic model is required in order to correctly account for the effect of the current.

1 INTRODUCTION

Design load cases on wind turbines comprise of computer simulations that predict the operational, extreme and shutdown loads of a wind turbine in its estimated lifetime. The design load cases are divided into fatigue design and ultimate design cases [1]. The fatigue design loads are to a greater extent determined by simulating turbine operation with normal turbulence wind input from cut-in to cut-out mean wind speeds. The expected value of the wave significant height and peak crossing period at each mean wind speed is used to simulate the hydrodynamic loads. Rainflow counting [2] algorithms process the load time series over all turbine components to determine damage equivalent loads. It is assumed that the limited number of simulations performed is reflective of the total life time of the turbine whereby the resulting accumulated damage can be computed.

Many model uncertainties are present in the computation of fatigue loads on wind turbine structures, which are subject to highly dynamic loads and are also lightly damped. Most model uncertainties [3] that are quantified in literature deal with the aero-hydro-elastic models used in loads simulations, the wind turbulence variations and the methods utilized in quantifying load cycles. Further there are also uncertainties in the S-N curves [4] that are used to predict failure, especially in the presence of grouted or welded joints as in the case of offshore sub structures. However, another key model uncertainty is the inclusion of mean effects in the damage equivalent load determination. Different offshore turbine design standards cite varying recommendations in this regard. For example, the DNV report DNV-RP-C203 [4] neglects the specific use of mean corrections in the damage equivalent load estimation. On the other hand, the GL guidelines [5] recommend considering the mean stress corrections in the determination of damage equivalent loads. The effects of mean stress on fatigue stress limits of steel structures has been classically evaluated using the Goodman method [6]. However, the this method tends to be over conservative and other approaches have been suggested which give superior results. Namely, the Walker [7] formula is shown to be specially suited for cases where the mean stress is relatively low [8]. The material parameter in the Walker model has been calibrated using an extensive database of experimental data. Empirical formulas have been suggested for its determination based on the material ultimate stress [8]. For cases where the mean is relatively large a formulation based on the mean stress sensitivity factor has been put forward [9]. Also here, a material dependent parameter is used based on the ultimate stress of the material. The mean value corrections suggested in the GL guidelines [5] are based on this concept.

Wind turbine support structure dynamics are strongly influenced by the rotor loads, but may also be affected by the marine loads. The marine loads play a greater role as the wind turbine is installed in deeper waters. As wind turbine installations move to moderate water depths of 35m and above, the hydrodynamic models play a significant role in the determination of support structure design loads. Conventional load simulation codes utilize linear irregular wave kinematics or nonlinear regular waves [10] to determine the design loads on offshore turbines, but at these moderate depths the wave kinematics is nonlinear and non Gaussian. Therefore herein a second order nonlinear irregular wave model is utilized to determine the hydrodynamic loads on the monopile structure installed at 35m water depth. The bandwidth of the energy spectra for nonlinear waves is greater than that of linear waves, which implies greater probability of wave excitation of the support structure that influences the fatigue loads. Monopile installations are largely been confined to less than 30m water depths presently, but their potential at water depths near 35m is to be explored.

2   METHODOLOGY

The methodology employed in the determination of the marine loads and analysis of the fatigue loads is presented in this section. Details of the nonlinear wave model including

sea current forces are discussed, following which, the different mean amplitude correction techniques considered in this paper are presented.

2.1 Determination of marine loads

The wave kinematics is modeled using second order irregular nonlinear waves, where the linear part of the wave free surface is derived from the JONSWAP spectrum [1] . The nonlinear wave model depicts a non Gaussian process whereby the first four stochastic moments of the process are utillized to simulate the waves to any time length using a polynomial chaos series expansion [11]. The wave kinematics is developed to predict the wave velocities and accelerations from the soil to the wave crest without utilizing any geometric stretching methods and by satisfying the wave free surface boundary conditions to the second order at each time instant in the time series simulation of waves. The wave acceleration and velocity are formulated as:

$$
\begin{aligned}
u = &\sum_{i=1}^{N} \frac{gk_i}{\omega_i} A_i \frac{\cosh(k_i(z+h))}{\cosh(k_i h)} \cos(k_i x - \omega_i t + \beta_i) \\
&+ \sum_{i=1}^{N} \sum_{j=1}^{M} B_j B_i \left[P_{ij} \cos(k_{ij}^- \chi - \omega_{ij}^- t + \beta_i) + Q_{ij} \cos(k_{ij}^+ \chi - \omega_{ij}^+ t + \beta_i) \right]
\end{aligned}
\tag{1}
$$

$$
\begin{aligned}
\dot{u} = &\sum_{i=1}^{N} -gk_i A_i \frac{\cosh(k_i(z+h))}{\cosh(k_i h)} \sin(k_i x - \omega_i t + \beta_i) \\
&+ \sum_{i=1}^{N} \sum_{j=1}^{M} C_j C_i \left[R_{ij} \sin(k_{ij}^- \chi - \omega_{ij}^- t + \beta_i) + S_{ij} \sin(k_{ij}^+ \chi - \omega_{ij}^+ t + \beta_i) \right]
\end{aligned}
\tag{2}
$$

Where B, C, P_{ij}, Q_{ij}, R_{ij}, and S_{ij} are terms dependent on the wave amplitude, frequency and wave number and require a fairly detailed formulation, which is provided in [11]. The superscripts $+$ and $-$ refer to a summation or difference between the frequencies ω_i, ω_j or between the wave numbers k_i, k_j. The forces on the sub-structure are computed using the Morison equation [1], which requires the evaluation of the wave velocity and acceleration normal to the structure. The wave loading at a section of the monopile is given by:

$$
dF(z,t) = C_M \rho \frac{\pi}{4} d^2 (\dot{u}_n - a_s) dz + C_d d \frac{1}{2} \rho (u_n - v_s) |u_n - v_s| dz
\tag{3}
$$

where C_M is the coefficient of inertia, d is the diameter of the monopile, u_n is the normal wave velocity at the section z, a_s is the structural acceleration, v_s is the structural velocity, and C_d is the coefficient of drag.

The presence of currents is common in wind farms, such as tidal currents and they may be in the same direction as the wave or even oppose it. Currents are normally considered
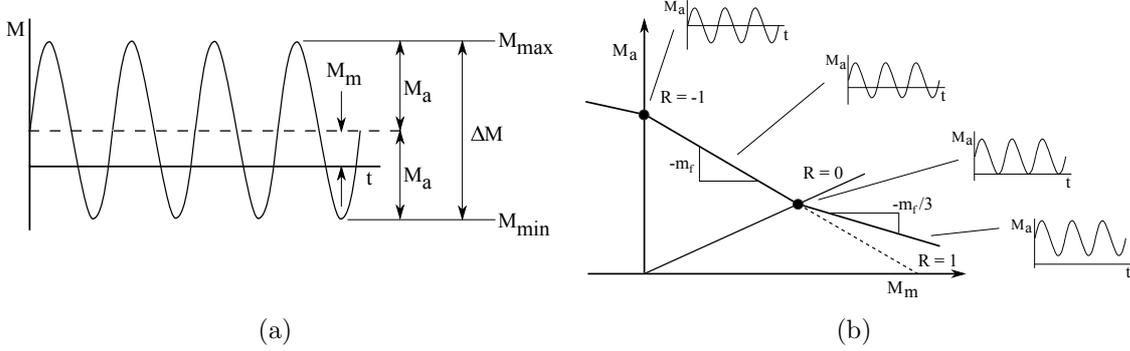
Figure 1: (a) Description of the cycle amplitude M_a, range ΔM, mean M_m, maximum M_{max}, and minimum M_{min}. (b) Haigh diagram showing magnitude of m_f and the mean and amplitude relation for different ranges of R.

not to impact the fatigue damage equivalent loads [1], but this is due to the assumption of linear wave kinematics, whereby the current only affects the mean drag force. Using the 2-D nonlinear Euler equations of fluid dynamics, Eq. (3) in the presence of currents can be re-written as

$$
\begin{aligned}
dF(z,t) = {} & C_M \rho \frac{\pi}{4} d^2 \left(\frac{\partial u}{\partial t} + (u+c)\frac{\partial u}{\partial x} + w\frac{\partial u}{\partial z} - a_s \right) dz \\
& + C_d d \frac{1}{2} \rho (c + u_n - v_s)|(c + u_n - v_s)| dz
\end{aligned}
\tag{4}
$$

where c is the constant current velocity, $\partial u/\partial x$ and $\partial u/\partial z$ are the derivatives of the normal velocity with displacement and $\partial u/\partial t$ is the local acceleration. From Eq. (4), it can be readily seen that the current velocity, though a constant affects the amplitude of the marine load and not just the mean. As the current velocity enters the inertial forcing term as a multiple of the spatial derivative, the current affects the amplitude of the inertial force, which implies it also affects the damage equivalent load directly. Since the mean of $\partial u/\partial x$ is zero, the mean inertial load is not affected by the current. However the mean drag force is increased due to the presence of the current. Hence using nonlinear waves, the current increases the mean drag force and also increases the amplitude of the inertial loads. The analysis suggested in the next section where the fatigue damage equivalent bending moment includes mean load amplitude corrections, will be able to account for both the mean and amplitude effects.

2.2 Fatigue damage analysis

The damage is assessed based on the mud line bending moment resulting from the wind, wave, and current forces. The fatigue analysis procedure typically based on stresses is herein based on the bending moment. Hence, where one would usually read *stress*, here it is mentioned *moment*.

4

The analysis of the fatigue damage in the monopile foundation is done in terms of the fatigue damage equivalent bending moment [9]. The fatigue damage D_i resulting from one load cycle of intensity M_i is given by $D_i = 1/N_i$ where N_i is the number of cycles to failure for a bending moment of intensity M_i. The accumulated damage from a varying number of cycles with different stress intensities is given by $D = \sum_{i=1}^{n_c} D_i = \sum_{i=1}^{n_c} n_i/N_i$. In the expression above, n_c is the total number of cycles, and n_i is the number of cycles for which N_i is the limit value at the corresponding bending moment level. The fatigue damage equivalent bending moment is given by

$$M_{eq} = \left(\frac{\sum_{i=1}^{n_b} n_i M_i^m}{N} \right)^{\frac{1}{m}} \tag{5}$$

where n_b is the number of bins used for the cycle counting, n_i and M_i are the number of cycles and moment intensity at bin i, respectively, m is the slope of the SN curve and is material dependent, and N is a predefined number of cycles.

For irregular load signals a cycle counting technique is usually employed to determine the amplitudes and means of the underlying load cycles. The rainflow cycle counting technique has been shown to match experimental results better [12] and an implementation of this algorithm is therefore used in this paper [13]. The rainflow cycle amplitudes are binned in order to determine the values of n_i and M_i which are then used in Eq. (5). The number of cycles counted from the load histories are further scaled by the Weibull hours for each mean wind speed to estimate the lifetime fatigue damage equivalent bending moment.

2.2.1   Mean value correction techniques

The properties of the SN curve are given assuming that the mean of the load cycles is low or negligible with respect to the amplitude. However, in some cases the mean load level may contribute to the fatigue damage. In order to account for mean load effects, different methods have been suggested in which the amplitudes of each cycle are corrected in function of its mean. For a given cycle amplitude and mean – M_a and M_m, respectively – an *equivalent reversed moment amplitude*, M_{ar}, is defined that is expected to cause the same life. Having determined M_{ar} it is possible to determine the mean corrected amplitude histograms and recompute the fatigue damage equivalent bending moments using Eq. (5).

Different mean load amplitude correction techniques with varying degree of accuracy are available in the literature. The accuracy and validity of the different techniques depends, among other, on the magnitude of R, defined here as

$$\begin{cases} R = \frac{M_{min}}{M_{max}}, & \text{iff} \quad M_m \geq 0 \\ R = \frac{M_{max}}{M_{min}}, & \text{iff} \quad M_m < 0 \end{cases} \tag{6}$$

where $M_{max} = M_m + M_a$, $M_{min} = M_m - M_a$. An alternative definition of R can be given in terms of the amplitude and mean of a given cycle as $M_m/M_a = (1+R)/(1-R)$. Different

R values correspond to different relations between cycle amplitude and mean as described in Figure 1(b). Note that the definition of R presented in (6) is different from that typically used for the stresses (see, e.g., Dowling et al [8]). A negative stress corresponds to compression in which case it is to expect that the fatigue life of the component is not increased. In this case it is correct to assume that R is always within the range $-1 \leq R \leq 1$.

Four different mean load correction techniques are considered in this study – Goodman, Walker, mean moment sensitivity factor, and a variation of the latter. The expression proposed by Goodman [6] is

$$M_{ar} = \frac{M_a}{1 - \frac{M_m}{M_u}} \tag{7}$$

where it is assumed that the ultimate bending moment $M_u = 1.5 M_{max}^T$ where M_{max}^T is the maximum bending moment measured throughout the entire time series across all wind speeds. The Goodman expression is characterized by its simplicity and works relatively well for tensile mean stress levels. However, its results maybe be inaccurate and this expression should only be used when none of the material fatigue properties are known [8]. Alternatively, the Walker formula [7] is commonly used for estimating the fatigue life of components and has been shown to give superior results [8]. It is defined as

$$M_{ar} = M_a \left(\frac{2}{1-R} \right)^{1-\gamma}, \text{ where, } \gamma = -0.0002\sigma_u + 0.8818 \tag{8}$$

where $\gamma \in [0, 1]$ is a material dependent parameter and σ_u is the material ultimate stress. The Walker approach is mostly suitable for relatively low mean stresses [9].For relatively large mean stresses an alternative approach has been proposed based on the mean stress sensitivity factor, m_f, or the slope of the line in the Haigh plot [9]. In this case M_{ar} is defined as

$$M_{ar} = M_a + m_f |M_m|, \text{ where, } m_f = 0.00035\sigma_u - 0.1 \tag{9}$$

The material parameter $m_f \in [0, +\infty]$ is determined based on an empirical model. For steel structures the value of m_f can be determined based on the ultimate strength (see, e.g., [9] and [2]). For the cases where $0 \leq R \leq 1$ or $M_m > M_a$, m_f is typically lower by a factor of 3 such that $m_{f,3} \approx m_f/3$ (see Figure 2.2). This is due to the fact that the fatigue damage due to cycles with a high mean and relatively low amplitude is lower than that predicted by m_f. GL [5] suggest the same correction when working with ductile steels. This formulation is henceforth referred to as the R-corrected mean moment sensitivity factor.

3 RESULTS

The analysis of the fatigue damage on the monopile foundation using mean value correction techniques is presented in this section. The setup of the numerical experiments

is described first. The resulting fatigue damage equivalent bending moments are compared and the effect of the amplitude corrections is analysed next. Finally, the effect of the currents is discussed.

3.1 Setup

The mud line bending moment time series acting on the monopile are simulated in HAWC2, an aero-hydro-elastic software [14], using the NREL 5MW wind turbine [15] mounted on a monopile foundation at 35m water depth. The loads are analysed for 18 different mean wind speeds ranging from 8m/s to 25m/s. Three random turbulent seeds are used for each mean wind speed. Each of the time series is 600 s long. The fore-aft (i.e., wind direction) and side-side (i.e., transverse to the wind direction) directions are treated separately. The results are determined with and without sea current which is collinear with the waves and acts in the fore-aft direction. The load time series are filtered using a rainflow cycle counting technique to identify the amplitude and mean of the equivalent load cycles [13]. A number of $n_b = 100$ bins is used for binning the rainflow cycle amplitudes and determine the number of cycles. The Weibull shape parameter is $\kappa = 2$, the mean value $\overline{w}_{wbl} = 10m/s$, and thus the scaling parameter is $\lambda = \overline{w}_{wbl}/\Gamma(1 + 1/\kappa) = 11.28$. The total number of load cycles for each mean wind speed throughout the 20 year lifetime are scaled from the corresponding Weibull hours.

It is assumed that the monopile foundation is built of steel NV-36 for which the stiffness modulus is E=210 Mpa, the shear modulus is G=80 Mpa and the ultimate stress is $\sigma_u = 550$ Mpa. The material dependent parameters used in the Walker Eq. (8) and mean moment sensitivity factor Eq. (9) determined based on the ultimate stress are $\gamma = 0.772$ and $m_f = 0.0925$, respectively. Moreover, for all cases a slope of the SN curve $m = 4$ is chosen. This is within the range between 3 and 5 typically chosen for this type of structures [5].

3.2 Discussion

The fore-aft and side-side lifetime fatigue damage equivalent bending moments with and without current and mean load corrections, are presented in Table 1. Note that the estimated values have an uncertainty associated with it due to the finite number of seeds. This is also the reason for the results in Figure 3 to be non-smooth. The distribution of the counted cycles in an amplitude versus mean histogram for the fore-aft and side-side loads with current is presented in Figures 2 (a) and (b), respectively. The results without current are indistinguishable and are therefore omitted. The mean of the bending moment for each mean wind speed is presented in Figures 2 (c) and (d). The effect of the mean load correction on the fore-aft and side-side lifetime fatigue damage equivalent bending moment with current included is shown in terms of mean wind speed in Figure 3. The results without current are very similar – the magnitudes are slightly lower but the relative differences are the same. The effect of varying m has been studied and is

Table 1: Results for the fore-aft and side-side lifetime fatigue damage equivalent bending moment, M_{eq}. Results with and without current – *Current* and *No current*, respectively. The mean load corrections according to Goodman (GDM), Walker (WLK), mean sensitivity factor (MSF), and R-corrected mean sensitivity factor (MSF/3), are considered. *rel. dif.* and *abs. dif.* refer to relative and absolute differences, respectively. *Orig. vs. Correct.* refers to a comparison between the original and mean corrected values. *Curr. vs. no curr.* refers to a comparison between the results with and without sea current forces.

Fore-aft		Original	GDM	WLK	MSF	MSF/3
No current	M_{eq} (kNm)	1.52E5	2.03E5	1.86E5	1.74E5	1.62E5
Orig. vs.	rel. dif. (%)	-	33.6	22.1	14.5	6.2
Correct.	abs. dif. (kNm)	-	5.12E4	3.36E4	2.20E4	9.42E3
Current	M_{eq} (kNm)	1.64E5	2.18E5	1.99E5	1.87E5	1.74E5
Orig. vs.	rel. dif. (%)	-	32.8	21.4	13.8	6.0
Correct.	abs. dif. (kNm)	-	5.37E4	3.52E4	2.26E4	9.92E3
Curr. vs.	rel. dif. (%)	7.3	6.7	6.8	6.7	7.1
no curr.	abs. dif. (kNm)	1.19E4	1.45E4	1.35E4	1.25E4	1.24E4

Side-side		Original	GDM	WLK	MSF	MSF/3
No current	M_{eq} (kNm)	3.76E4	4.24E4	4.26E4	4.03E4	3.96E4
Orig. vs.	rel. dif. (%)	-	12.9	13.3	7.2	5.2
Correct.	abs. dif. (kNm)	-	4.84E3	5.02E3	2.69E3	1.97E3
Current	M_{eq} (kNm)	3.78E4	4.26E4	4.28E4	4.05E4	3.98E4
Orig. vs.	rel. dif. (%)	-	12.9	13.3	7.1	5.2
Correct.	abs. dif. (kNm)	-	4.87E3	5.02E3	2.68E3	1.97E3
Curr. vs.	rel. dif. (%)	0.5	0.5	0.4	0.4	0.5
no curr.	abs. dif. (kNm)	1.84E2	2.16E2	1.87E2	1.75E2	1.86E2

presented in Figure 4 where it is assumed that $\overline{w}_s = 16$ m/s. Finally, the effect of the current on the magnitudes of the lifetime fatigue damage equivalent bending moment is visible in Figure 5.

From Table 1 we can see that the effect of the mean load amplitude corrections is more significant in the fore-aft than in the side-side loads. This is in agreement with the results from Figures 2 (c) and (d) which show that the mean of the bending moment of the fore-aft loads is significantly higher. The negative mean values measured in the side-side loads are most probably due to the moment induced by the generator as it counteracts the rotor torque.

In the fore-aft case the R-corrected mean sensitivity factor (MSF/3), mean sensitivity factor (MSF), Walker (WLK), and Goodman (GDM) techniques give increasingly conservative results (see Table 1). The same trend is observed in Figure 3 where it is also clear that the difference between the mean corrected and uncorrected results is larger at lower wind speeds. As can be observed in Figure 2 (a), for most of the load cycles
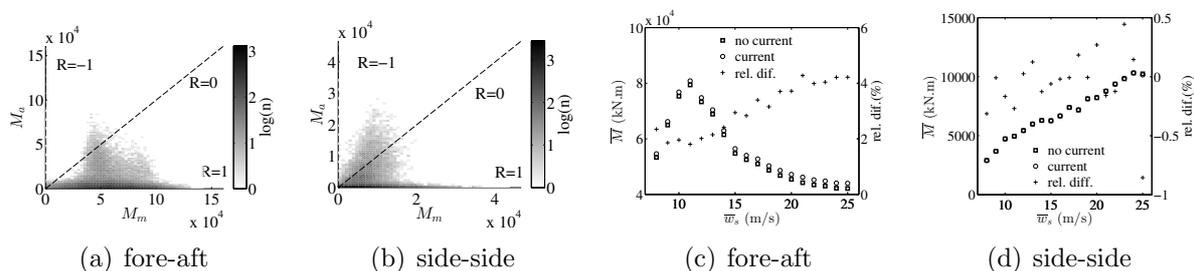
Figure 2: Histogram of amplitude M_a versus mean M_m for the fore-aft (a) and side-side (b) mud line bending moment with sea current included for all wind speeds. Gray scale indicates number of cycles n in each bin (log scale). Fore-aft (c) and side-side (d) mean mud line bending moment, $\overline{M}$, with and without current for different mean wind speeds, $\overline{w}_s$.
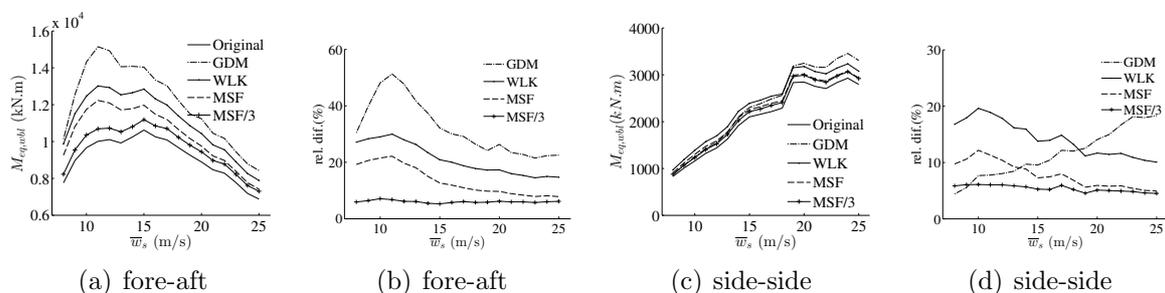

Figure 3: Comparison between the fatigue damage equivalent bending moments, M_{eq}, scaled by the Weibull hours for different mean wind speeds, $\overline{w}_s$. Results with and without mean value moment corrections based on Goodman (GDM), Walker (WLK), mean moment sensitivity factor (MSF), and R-corrected mean moment sensitivity factor (MSF/3). Results for $m = 4$ and $N_{eq} = 1 \times 10^6$ cycles. Magnitude (a-c) and relative difference (b-d) of fore-aft and side-side fatigue damage equivalent bending moment.

across all wind speeds the ratio R (from Eq. (6)) is within the range $0 < R < 1$. It is therefore to expect that techniques which are tailored for this type of loads (i.e., MSF and MSF/3) give less conservative results than others developed to work with lower R values (i.e., WLK and GDM). Moreover, the higher values of M_{eq} at lower wind speeds are in agreement with the results from Figure 5 which show that the mean bending moment is higher within this range. Regarding the effect of varying m, there is an asymptotic trend for WLK, MSF, and MSF/3 for which the relative difference remains constant for $m > 5$ (see Figure 4). Below this value and for these three techniques, the error grows rapidly. The relative difference for the GDM case is constant for all mean wind speeds.

The same trend between the different mean correction techniques is observed in the side-side case although here the GDM and WLK results are closer. The variation of the lifetime fatigue damage equivalent bending moment for the different wind speed is also similar except for the GDM case which presents an increasing relative difference with increasing wind speeds (see Figure 3 (d)). Finally the effect of varying m is also very similar although the GDM case is less conservative than the WLK for a wider range of
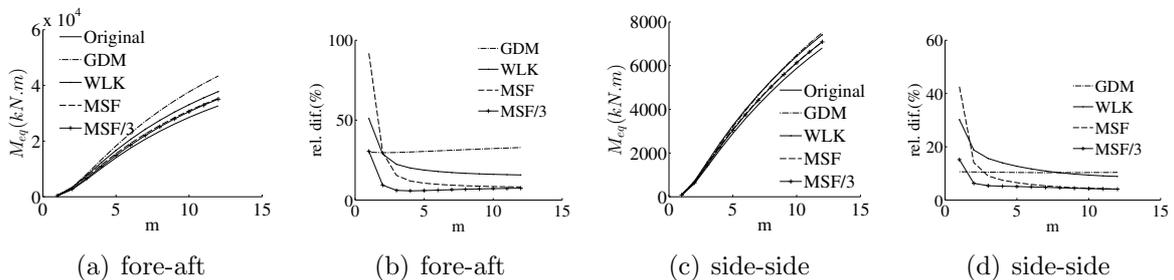
(a) fore-aft   (b) fore-aft   (c) side-side   (d) side-side

Figure 4: Comparison between the fatigue damage equivalent bending moments, M_{eq}, for different values of m including sea current forces. Results with and without mean value moment corrections based on Goodman (GDM), Walker (WLK), mean moment sensitivity factor (MSF), and R-corrected mean moment sensitivity factor (MSF/3). Results for $\overline{w}_s = 16m/s$ and $N_{eq} = 1 \times 10^6$ cycles. Magnitude (a-c) and relative difference (b-d) of fore-aft and side-side fatigue damage equivalent bending moment.

wind speeds.

The effect of the current on the lifetime fatigue damage equivalent bending moment is expected to be null if the current affects only the mean of the loads. However, from Table 1 and Figure 5, it is seen that the results with and without current are different which shows that the amplitudes are also affected by the current. A simple experiment can reveal the effect of the sea current in terms of the amplitude and mean separately. For each mean wind speed the load histories determined without sea current are offset exactly by the mean of the corresponding results with current. This mimics the case where the sea current affects only the mean. As expected, the value of the fatigue damage equivalent bending moment without mean load correction remains the same as the amplitudes remain unchanged. The mean corrected values, on the other hand, present very small differences (approximately 0.5%) independently of the correction technique. These results emphasize the fact that the effect of the sea current in the load cycle amplitudes is the most important contribution to the increase in fatigue damage equivalent bending moment. Most importantly, this effect can only be correctly accounted for if the nonlinear model of the marine loads as in Eq. (4) is used.

Finally, it is noted that the relative difference between the results with and without current is smaller when using mean load amplitude correction techniques. This seems to suggest that the mean correction techniques reduce the effect of the current. However, the absolute differences are larger which is in agreement with the expected trend.

4   CONCLUSIONS

The mud line bending moment acting on the monopile is determined using an aero-hydro-elastic model which accounts for nonlinear wave and sea current effects. The fatigue damage is analysed in terms of the fore-aft and side-side lifetime fatigue damage equivalent bending moment with and without sea current forces. Four different mean load amplitude correction techniques are compared - Goodman (GDM), Walker (WLK), the
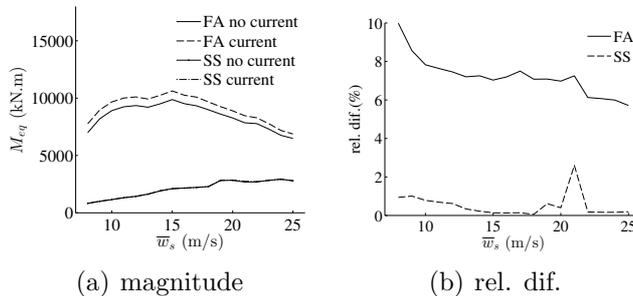
(a) magnitude   (b) rel. dif.

Figure 5: Magnitude (a) and relative difference (b) of the fore-aft (FA) and side-side (SS) fatigue damage equivalent bending moments, M_{eq}, with and without current for different mean wind speeds, $\overline{w}_s$. Results obtained without mean moment amplitude correction for $m = 4$ and $N_{eq} = 1 \times 10^6$ cycles.

mean moment sensitivity factor (MSF), and the R-corrected mean moment sensitivity factor (MSF/3). Increases in the lifetime fatigue damage equivalent bending moment ranging from approximately 6% (MSF/3) to 30% (GDM) are observed. These results demonstrate the importance of using mean load amplitude correction techniques in the design of monopile foundations. Furthermore, it is also shown that for most of the load cycles the ratio R between the minimum and maximum of each cycle is $0 < R < 1$. This suggests that MSF and MSF/3, which are designed to work in this range of R, are probably the most suitable. Finally, an increase of approximately 7% in the fore-aft lifetime fatigue damage equivalent bending moment due to the sea current is observed. It is shown that this difference is mostly motivated by an increase in the amplitude and not the mean of the load cycles. This result is a clear indication that a nonlinear wave model is required in order to correctly account for the sea current effects.

REFERENCES

[1] IEC International Standard, *Wind Turbines Part 3, Design requirements for offshore wind turbines*, Edition 1, 2009.

[2] Veldkamp, H.F. *Chances in Wind Energy - a Probabilistic approach to wind turbine fatigue design.* Ph.D. Thesis, Delft University, (2006).

[3] Sørensen J.D., Frandsen F., Tarp-Johanssen N.J., Effective turbulence models and fatigue reliability in wind farms, *Journal of Probabilistic Engineering Mechanics.* (2008) **23**(4):531–538.

[4] DNV Recommended Practice, *Fatigue Design of Offshore Steel Structures*, Report number DNV-RP-C203, (2011).

[5] GL Rules and Guidelines, *Guidelines for the certification of wind turbines.* Germainscher Lloyd Industrial Services Gmbh, July 1st, (2010).

[6] Goodman, J. *Mechanics applied to engineering*. Longmans, Green and Co., London, (1919).

[7] Walker, K. The effect of stress ratio during crack propagation and fatigue for 2024-T3 and 7075-T6 aluminum. *Effects of environment and complex load history on fatigue life, ASTM STP 462* (1970) Philadephia, PA, 1–14.

[8] Dowling, N. E. and Calhoun, C. A. and Arcari, A. Mean stress effects in stress-life fatigue and the Walker equation. *Fatigue & Fracture of Engineering Materials & Structures* (2009) **32**(3):163–179.

[9] Lee, Y.L., Pan, J., Hathaway, R., Barkley, M. *Fatigue testing and analysis - theory and practice*. Elsevier, (2005).

[10] De Wries W., Vemula N.K., Passon P., Fischer T., Kaufer D., Matha D., Schmidt B., Vorpahl F. *Support Structure Concepts for Deep Water Sites*. UpWind Project final report D4.2.8, (2011).

[11] Moan T., Zheng X.Y., Quek S.T. Frequency-domain analysis of non-linear wave effects on offshore platform responses. *International Journal of Non-Linear Mechanics* (2007) **42**:555–565.

[12] Dowling, N.E. Fatigue predictions for complicated stress-strain histories. *J. Materials* (1972) **7**:71–87.

[13] WAFO-group, WAFO - A Matlab Toolbox for Analysis of Random Waves and Loads - A Tutorial., Math. Stat., Center for Math. Sci., Lund Univ., Lund, Sweden, (2000).

[14] Larsen, T.J., Hansen, A.M., *How 2 HAWC2, the user's manual*. Technical University of Denmark, (2006).

[15] Jonkman, J., Butterfield, S., Musial, W., Scott, G., *Definition of a 5-MW reference wind turbine for offshore system development*. NREL/TP-500-38060, (2009).